This article was downloaded by: [Renmin University of China]
On: 13 October 2013, At: 10:48
Publisher: Taylor & Francis
Informa Ltd Registered in England and Wales Registered Number: 1072954 Registered office: Mortimer House, 37-41 Mortimer Street, London W1T 3JH, UK

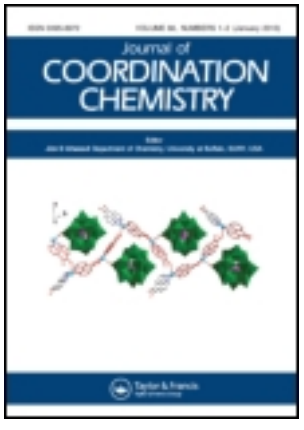

Journal of Coordination Chemistry
Publication details, including instructions for authors and subscription information:
http://www.tandfonline.com/loi/gcoo20

3,6-Bis(1H-1,2,3,4-tetrazol-5-yl-amino)-1,2,4,5-tetrazine-based energetic strontium(II) complexes: synthesis, crystal structure, and thermal properties

Xian-Bo Zhang [a], Ying-Hui Ren [a b], Wen Li [a], Feng-Qi Zhao [b], Jian-Hua Yi [a], Bo-Zhou Wang [a] & Ji-Rong Song [a c]

[a] Shaanxi Key Laboratory of Physico-inorganic Chemistry, School of Chemical Engineering, Northwest University, Xi'an, PR China

[b] Science and Technology on Combustion and Explosion Laboratory, Xi'an Modern Chemistry Research Institute, Xi'an, PR China

[c] Conservation Technology Department, The Palace Museum, Beijing, PR China

Accepted author version posted online: 16 Apr 2013.Published online: 24 May 2013.

To cite this article: Xian-Bo Zhang, Ying-Hui Ren, Wen Li, Feng-Qi Zhao, Jian-Hua Yi, Bo-Zhou Wang & Ji-Rong Song (2013) 3,6-Bis(1H-1,2,3,4-tetrazol-5-yl-amino)-1,2,4,5-tetrazine-based energetic strontium(II) complexes: synthesis, crystal structure, and thermal properties, Journal of Coordination Chemistry, 66:12, 2051-2064, DOI: 10.1080/00958972.2013.796040

To link to this article: http://dx.doi.org/10.1080/00958972.2013.796040

PLEASE SCROLL DOWN FOR ARTICLE

Taylor & Francis makes every effort to ensure the accuracy of all the information (the "Content") contained in the publications on our platform. However, Taylor & Francis, our agents, and our licensors make no representations or warranties whatsoever as to the accuracy, completeness, or suitability for any purpose of the Content. Any opinions and views expressed in this publication are the opinions and views of the authors, and are not the views of or endorsed by Taylor & Francis. The accuracy of the Content should not be relied upon and should be independently verified with primary sources of information. Taylor and Francis shall not be liable for any losses, actions, claims, proceedings, demands, costs, expenses, damages, and other liabilities whatsoever or

howsoever caused arising directly or indirectly in connection with, in relation to or arising out of the use of the Content.

This article may be used for research, teaching, and private study purposes. Any substantial or systematic reproduction, redistribution, reselling, loan, sub-licensing, systematic supply, or distribution in any form to anyone is expressly forbidden. Terms & Conditions of access and use can be found at http://www.tandfonline.com/page/terms-and-conditions

Downloaded by [Renmin University of China] at 10:48 13 October 2013

Journal of Coordination Chemistry, 2013
Vol. 66, No. 12, 2051–2064, http://dx.doi.org/10.1080/00958972.2013.796040

Taylor & Francis
Taylor & Francis Group

Downloaded by [Renmin University of China] at 10:48 13 October 2013

3,6-Bis(1H-1,2,3,4-tetrazol-5-yl-amino)-1,2,4,5-tetrazine–based energetic strontium(II) complexes: synthesis, crystal structure, and thermal properties

XIAN-BO ZHANG†, YING-HUI REN†‡*, WEN LI†, FENG-QI ZHAO‡, JIAN-HUA YI†, BO-ZHOU WANG† and JI-RONG SONG†§

†Shaanxi Key Laboratory of Physico-inorganic Chemistry, School of Chemical Engineering, Northwest University, Xi'an, PR China
‡Science and Technology on Combustion and Explosion Laboratory, Xi'an Modern Chemistry Research Institute, Xi'an, PR China
§Conservation Technology Department, The Palace Museum, Beijing, PR China

(*Received 6 December 2012; in final form 14 February 2013*)

Two energetic strontium(II) complexes with nitrogen-rich 3,6-bis(1H-1,2,3,4-tetrazol-5-yl-amino)-1,2,4,5-tetrazine (BTATz) were synthesized. The metal complexes were characterized by IR, elemental analysis, and single-crystal X-ray diffraction. DSC and TG-DTG were used to study the thermal behavior, non-isothermal decomposition reaction kinetics, self-accelerating decomposition temperature (T_{SADT}), thermal ignition temperature (T_{TIT}), critical temperature of thermal explosion (T_b), and the adiabatic time-to-explosion (t_{TIad}). The data indicate competitive energetic materials.

Keywords: 3,6-Bis(1H-1,2,3,4-tetrazol-5-yl-amino)-1,2,4,5-tetrazine; Crystal structure; Strontium; Non-isothermal kinetics; Thermal safety

1. Introduction

3,6-Bis(1H-1,2,3,4-tetrazol-5-yl-amino)-1,2,4,5-tetrazine (BTATz) was first synthesized by Hiskey *et al*. at Los Alamos National Laboratory [1]. Because of its advantageous properties [1–8], it is regarded as a new high-energy explosive; it was also used as fire suppressing gas generators. The burning rate can be improved with the substitution of RDX (1,3,5-trinitro-1,3,5-triazacyclohexane) or HMX (1,3,5,7-tetranitro-1,3,5,7-tetrazocane) by BTATz in the CMDB propellant formulation [5, 9].

High energy metal salts have attracted immense attention, used as one component of the explosives and propellants [10, 11], and also play an important role as energetic catalysts [12–14]. Burning rate of salts is highly dependent on the position of the metal [15] and the thermal stability of energy materials has an important relationship with the ligands. So, structure–properties relationship for the metal salts of BTATz is of interest. Researchers have found that carbon materials have a positive effect in increasing the burning rate [16]. Conjugated compound, such as 1,10-phenanthroline and BTATz in a complex can reduce the sensitivity.

*Corresponding author. Email: nwuryh@163.com

© 2013 Taylor & Francis

In this paper, $K_2(BTATz)\cdot 2H_2O$ as an intermediate was synthesized by the poor acidity of BTATz and strong alkalinity of KOH. Then two strontium complexes of $Sr_2(BTATz)_2(H_2O)_8\cdot 3H_2O$ and $Sr(BTATz)(phen)(H_2O)_4\cdot H_2O$ were synthesized and their crystal structures were determined. Their thermal behavior and thermal safety were studied by DSC and TG-DTG techniques.

2. Experimental

2.1. *Reagents and apparatus*

All chemicals used in the synthesis were of analytical grade commercial products and used without purification. BTATz was provided by Xi'an Modern Chemistry Research Institute (purity, 99.9%) [8]. Elemental analysis was performed on a VarioELIII elemental analyzer (Elementar Co., Germany). The content of Sr was determined on an S4 Pioneer X-ray fluorescence spectrometer (Bruker Co., Germany). IR spectrum was determined on EQUINX55 with KBr pellets. The crystal structure was obtained on a Bruker SMART APEX II X-ray diffractometer. TG-DTG and DSC curves were obtained under flowing nitrogen (purity, 99.999%; atmospheric pressure) using a SDTQ600 thermal analyzer (TA Co., USA). The specific heat capacities (C_p) of the two complexes were determined using a micro-DSC III apparatus (SETARAM, France), the amounts of used samples were 350 mg, and the heating rate was $0.15\,K\,min^{-1}$ ($2.5\times10^{-3}\,K\,s^{-1}$) from 283.15 to 353.15 K.

2.2. *Synthesis of $K_2(BTATz)\cdot 2H_2O$*

A solution of KOH (0.2244 g in 10 mL of distilled water) was added dropwise into the solution of BTATz (0.4960 g, 2 mM) in DMF (20 mL). The reaction mixture was stirred at 333.15 K for 5 h. The solvent was evaporated and the amaranth precipitate was collected by filtration, washed with ethanol and dried at 323.15 K, yielding 63.0%. Anal. Calcd for $C_4H_6N_{14}O_2K_2$ (%): C, 13.33; N, 54.41; H, 1.68. Found: C, 13.99; N, 54.51; H, 1.499. IR (KBr, ν/cm^{-1}): 3379, 3232 (N–H), 3016, 2853, 1687, 1587 (C–N), 1440 (N–N), 1046, 960, 783.

2.3. *Synthesis of $Sr_2(BTATz)_2(H_2O)_8\cdot 3H_2O$ (1)*

Complex **1** was synthesized with the diffusion method. A solution of $Sr(NO_3)_2$ (0.1 mM in 10 mL of distilled water) was added dropwise into a test tube, then 5 mL distilled water was layered on top. Afterwards, a solution of $C_4H_6N_{14}O_2K_2$ (0.1 mM in 10 mL of distilled water) was added dropwise slowly to the water layer. Single crystals suitable for X-ray measurement were obtained after one week at room temperature. Anal. Calcd for $C_8H_{18}N_{28}O_{11}Sr_2$ (%): C, 11.20; N, 45.73; H, 2.12; Sr, 20.43. Found: C, 11.80; N, 47.63; H, 2.32; Sr, 19.62. IR (KBr, ν/cm^{-1}): 3533 (O–H), 3255 (N–H), 3028, 2825, 1621, 1520 (C–N), 1496 (N–N), 1062, 799.

Downloaded by [Renmin University of China] at 10:48 13 October 2013

Downloaded by [Renmin University of China] at 10:48 13 October 2013

2.4. *Synthesis of Sr(BTATz)(phen)(H_2O)$_4$·H_2O (2)*

Complex 2 was obtained by similar procedures to 1. A solution of $Sr(NO_3)_2$ (0.1 mM in 10 mL of distilled water) was added dropwise into a test tube, then 10 mL distilled water was added as a blank layer. A mixed solution of distilled water and ethanol (1 : 1 v/v) with $C_4H_6N_{14}O_2K_2$ (0.1 mM) and 1,10-phenanthroline (phen, 0.1 mM) was added dropwise slowly onto the blank layer. Then the test tube was placed in a black box and single crystals suitable for X-ray measurement were obtained after two weeks. Anal. Calcd for $C_{16}H_{20}N_{16}O_5Sr$ (%): C, 31.81; N, 37.10; H, 3.34; Sr, 14.51. Found: C, 30.22; N, 36.56; H, 3.12; Sr, 13.10. IR (KBr, ν/cm^{-1}): 3552 (O–H), 3415, 3255 (N–H), 3012, 2817, 1621, 1492 (N–N), 1407, 1058, 792, 556.

2.5. *Determination of the crystal structure*

A crimson prism-shaped single crystal (0.31 mm × 0.24 mm × 0.13 mm) of **1** and a red bulk-shaped single crystal (0.37 mm × 0.26 mm × 0.14 mm) of **2** were selected. Single crystal X-ray intensities were recorded by a Bruker SMART APEX II X-ray diffractometer using Mo$K\alpha$ radiation ($\lambda = 0.071073$ nm) graphite monochromated. The crystal structure was solved by direct methods [17] (SHELXTL-97) and refined by full-matrix-block least-squares on F^2 with anisotropic thermal parameters for all non-hydrogen atoms. Hydrogens were added according to the theoretical models. The crystal data have been deposited in Cambridge Crystallographic Data Center (CCDC) with the numbers of 887783 and 887784. The basic crystal data results are summarized in table 1.

Table 1. Crystal data and structure refinement details.

Complex	**1**	**2**
Chemical formula	$C_8H_{22}N_{28}O_{11}Sr_2$	$C_{16}H_{20}N_{16}O_5Sr$
Formula weight (g mol^{-1})	861.65	604.10
Temperature/K	296(2)	296(2)
Crystal system	Triclinic	Triclinic
Space group	*P* − *1*	*P* − *1*
a/Å	8.6524(16)	6.9305(14)
b/Å	10.112(2)	10.296(2)
c/Å	11.004(3)	17.171(4)
α	110.419(4)	86.264(4)
β	95.110(4)	87.143(4)
γ	111.777(3)	71.531(3)
Volume/Å^3	811.0(3)	1159.1(4)
Z	2	2
D_{calc}/g cm^{-3}	1.883	1.731
Absorption coefficient/mm^{-1}	3.393	2.394
F (0 0 0)	464	612
θ range (°)	2.62–22.76	2.38–21.11
Index ranges	$-10 \le h \le 10$, $-8 \le k \le 12$, $-12 \le l \le 13$	$-8 \le h \le 7$, $-12 \le k \le 8$, $-20 \le l \le 19$
Reflections collected/unique	2855/2396 [$R_{int} = 0.026$]	4097/2907 [$R_{int} = 0.032$]
Goodness-of-fit on F^2	1.021	1.002
Final *R* indices [$l > 2\sigma(l)$]	$R_1 = 0.0481$, wR_2=0.1262	$R_1 = 0.0610$, $wR_2 = 0.1338$
R indices (all data)	$R_1 = 0.0620$, $wR_2 = 0.1489$	$R_1 = 0.0935$, $wR_2 = 0.1541$
Largest diff. peak and hole (e Å^{-3})	0.622 and −0.811	1.151 and −0.755

Downloaded by [Renmin University of China] at 10:48 13 October 2013

3. Results and discussion

3.1. *Crystal structure*

Selected bond lengths and angles for **1** and **2** are listed in table 2.

Crystal structure (figure 1) analysis of **1** shows that there are two symmetry equivalent positions within the unit cell due to the presence of an inversion center. Both Sr have identical environments, eight coordinate with three nitrogens (N7, N11, N12A or N7A, N11A, N12) of two $BTATz^{2-}$ and five oxygens (O2, O2A, O3, O4, O5 or O2, O2A, O3A, O4A, O5A) of coordinated water. The bond lengths of strontium and five oxygens are between 2.559(4) and 2.656(4) Å with an average of 2.616 Å. The Sr–N bond lengths are 2.766(4), 2.768(5), and 2.768(5) Å. All are similar to those of alkaline-earth metal complexes [18, 19].

In $Sr_2(BTATz)_2(H_2O)_8{\cdot}3H_2O$, monodentate BTATz is coordinated with Sr(II) through N of tetrazine and tetrazole rings, little different to the result given by Ma's theoretical study

Table 2. Bond lengths [Å] and angles [°] for **1** and **2**.

Bond	Dist.	Bond	Dist.
Complex **1**			
Sr(1)–O(5)	2.559(4)	Sr(1)–N(11)	2.766(4)
Sr(1)–O(4)	2.608(4)	Sr(1)–N(12)#1	2.768(5)
Sr(1)–O(2)#1	2.628(4)	N(12)–Sr(1)#1	2.768(5)
Sr(1)–O(2)	2.656(4)	O(2)–Sr(1)#1	2.628(4)
Angle	(°)	Angle	(°)
O(5)–Sr(1)–O(4)	73.86(13)	O(4)–Sr(1)–N(12)#1	107.67(16)
O(5)–Sr(1)–O(3)	75.52(15)	O(3)–Sr(1)–N(12)#1	99.83(15)
O(4)–Sr(1)–O(3)	134.17(13)	O(2)#1–Sr(1)–N(12)#1	69.13(13)
O(5)–Sr(1)–O(2)#1	125.20(14)	O(2)–Sr(1)–N(12)#1	68.09(14)
O(4)–Sr(1)–O(2)#1	73.70(12)	N(11)–Sr(1)–N(12)#1	122.18(13)
O(3)–Sr(1)–N(11)	99.47(15)	C(4)–N(11)–Sr(1)	135.5(3)
O(2)#1–Sr(1)–N(11)	68.43(13)	N(12)–N(11)–Sr(1)	120.0(3)
O(2)–Sr(1)–N(11)	67.75(13)	N(13)–N(12)–Sr(1)#1	131.8(3)
O(5)–Sr(1)–N(12)#1	80.41(13)	N(11)–N(12)–Sr(1)#1	117.7(3)
Complex **2**			
Sr(1)–O(1)	2.536(6)	Sr(1)–N(6)#2	2.672(5)
Sr(1)–O(4)#1	2.585(5)	Sr(1)–N(2)#1	2.735(5)
Sr(1)–O(5)	2.610(4)	Sr(1)–N(1)#1	2.756(6)
Sr(1)–O(8)#1	2.622(4)	Sr(1)–N(8)#2	2.818(5)
Angle	(°)	Angle	(°)
O(1)–Sr(1)–O(4)#1	147.70(19)	N(6)#2–Sr(1)–N(2)#1	149.31(16)
O(1)–Sr(1)–O(5)	70.85(19)	O(1)–Sr(1)–N(1)#1	73.2(2)
O(4)#1–Sr(1)–O(5)	78.02(15)	O(4)#1–Sr(1)–N(1)#1	130.49(16)
O(1)–Sr(1)–O(8)#1	139.94(19)	O(5)–Sr(1)–N(1)#1	116.17(15)
O(4)#1–Sr(1)–O(8)#1	72.28(14)	O(8)#1–Sr(1)–N(1)#1	72.64(15)
O(5)–Sr(1)–O(8)#1	144.92(14)	N(6)#2–Sr(1)–N(1)#1	90.88(18)
O(1)–Sr(1)–N(6)#2	79.9(2)	N(2)#1–Sr(1)–N(1)#1	60.28(16)
O(4)#1–Sr(1)–N(6)#2	116.05(19)	O(1)–Sr(1)–N(8)#2	84.4(2)
O(5)–Sr(1)–N(6)#2	130.65(15)	O(4)#1–Sr(1)–N(8)#2	80.16(14)
O(8)#1–Sr(1)–N(6)#2	80.29(15)	O(5)–Sr(1)–N(8)#2	76.49(14)
O(1)–Sr(1)–N(2)#1	99.6(2)	O(8)#1–Sr(1)–N(8)#2	115.34(14)
O(4)#1–Sr(1)–N(2)#1	80.63(15)	N(6)#2–Sr(1)–N(8)#2	61.55(16)
O(5)–Sr(1)–N(2)#1	76.04(14)	N(2)#1–Sr(1)–N(8)#2	149.14(15)
O(8)#1–Sr(1)–N(2)#1	81.04(13)	N(1)#1–Sr(1)–N(8)#2	147.42(16)

Symmetry transformations used to generate the equivalent atoms: complex **1**: #1: $1-x$, $-y+1$, $-z+1$; complex **2**: #1: $x1$, y, z; #2: x, $y+1$, z.

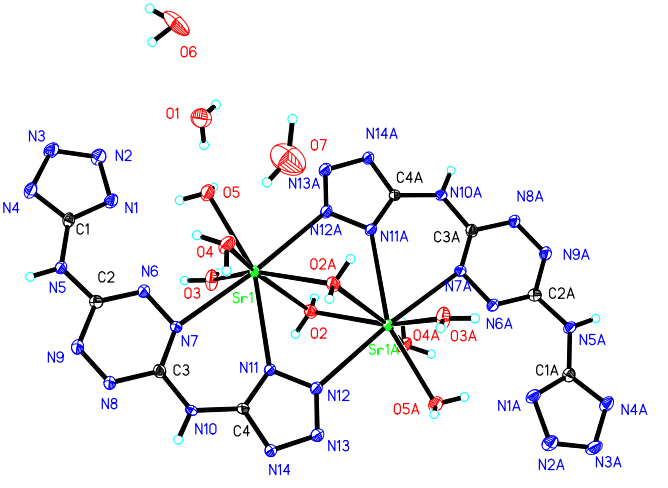

Figure 1. Molecular structure of **1**.

[20]. Two neighboring Sr ions link with two oxygens of two different waters into a circle forming a dinuclear unit.

A six-number ring was formed by two Sr(II) and four N (N11, N12, N11A, and N12A). The bond angles of N(11)–Sr(1)–N(12)#1, N(12)–N(11)–Sr(1), and N(11)–N(12)–Sr(1)#1 are 122.18(13), 120.0(3), and 117.7(3)°, respectively, which indicate that the ring has good planarity; the plane equation is $5.224x - 8.506y + 6.810z = -1.0544$.

As shown in the packing diagram of $Sr_2(BTATz)_2(H_2O)_8 \cdot 3H_2O$ (figure 2), many hydrogen bonds between N and O or O and O formed to link molecules into a 3-D network. table 3 summarizes the hydrogen bond parameters. H_2O plays an important role connecting $BTATz^{2-}$ and $Sr_2(BTATz)_2(H_2O)_8 \cdot 3H_2O$ via intermolecular hydrogen bonds, such as N5–H5A···O1#1, O6-H6B···N9#8, and N10-H10A···N14#2. Intramolecular hydrogen bonds

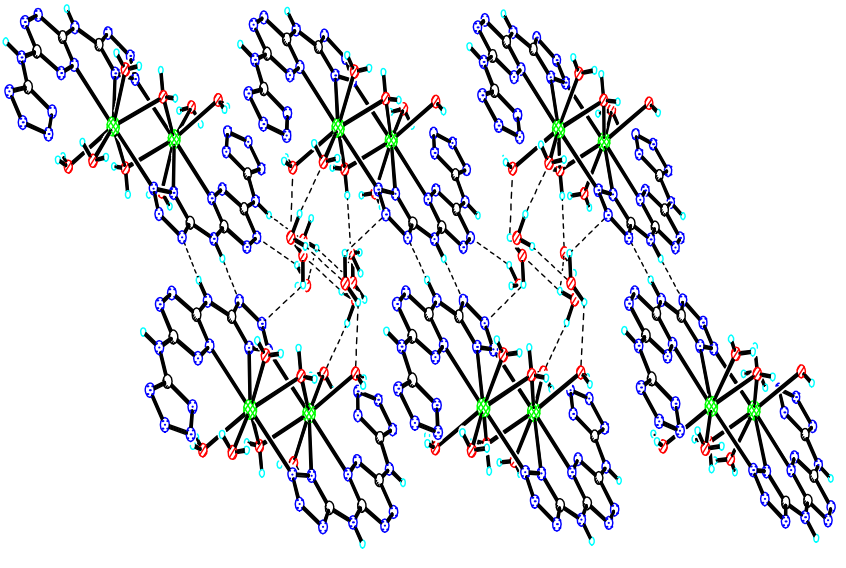

Figure 2. Packing diagram of **1** viewed along the *a*-axis.

Downloaded by [Renmin University of China] at 10:48 13 October 2013

Downloaded by [Renmin University of China] at 10:48 13 October 2013

Table 3. Hydrogen bonds for **1** and **2** (Å and °).

D–H···A	d(D–H)	d(H···A)	d(D···A)	∠(DHA)	D–H···A	d(D–H)	d(H···A)	d(D···A)	∠((DHA)
Complex **1**									
N5–H5A···O1#1	0.860	2.121	2.971	169.56	O4–H4B···N2#7	0.840	2.678	3.302	132.26
N10–H10A···N14#2	0.860	2.034	2.881	168.20	O5–H5B···N1	0.820	1.903	2.704	165.25
O1–H1B···O7#3	0.820	2.166	2.923	149.87	O5–H5B···N2	0.820	2.567	3.298	149.03
O3–H3A···N13#4	0.840	2.076	2.890	163.20	O2–H2B···O6#7	0.840	1.945	2.755	162.13
O3–H3B···O5#5	0.840	2.112	2.856	150.92	O6–H6B···O3#4	0.840	2.586	3.035	114.74
O4–H4A···N4#6	0.840	2.088	2.790	140.89	O6–H6B···N9#8	0.840	2.637	3.023	111.45
O4–H4B···N3#7	0.840	2.002	2.807	160.38	O7–H7B···O4	0.840	2.291	2.799	125.17
Complex **2**									
N7–H7···N3#1	0.860	2.127	2.938	157.03	O8–H88D···O4	0.840	2.319	3.071	141.01
N12–H12···N13#2	0.860	2.067	2.893	160.80	O4–H88A···N15	0.900	2.047	2.890	155.51
O1–H88I···N5#3	0.820	2.543	3.169	134.17	O4–H88B···N9#3	0.900	2.669	3.163	115.60
O2–H88E···N4#1	0.840	2.183	2.741	123.87	O5–H88G···O8	0.900	2.311	2.925	125.33
O2–H88F···O8	0.840	2.027	2.764	141.61	O5–H88H···N14	0.820	2.227	3.016	161.60
O2–H88F···N5#3	0.840	2.583	3.051	113.12					

Symmetry transformations used to generate the equivalent atoms: Complex **1**: #1: $-x-1, -y, -z$; #2: $-x-1, -y, -z$; #3: $-x+1, -y+2, -z+1$; #4: $x+1, y, z$; #5: $-x+1, -y+1, -z+1$; #6: $-x+1, -y+1, -z$; #7: $x-1, y, z$; #8: $-x+1, -y, -z$. Complex **2**: #1: $-x+2, -y, -z$; #2: $-x+1, -y, -z+1$; #3: $x-1, y+1, -z$; #4: $-x+1, -y+1, -z+1$.

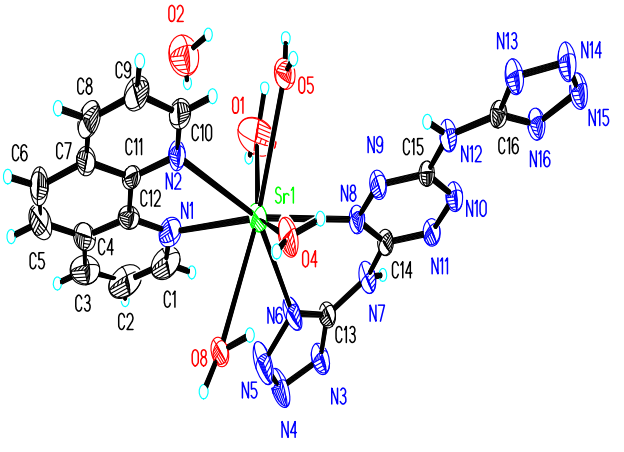

Figure 3. Molecular structure of **2**.

are found in lattice waters. The hydrogen bonding interactions make important contributions to stability of **1**.

Complex **2** has an asymmetric unit consisting of one Sr^{2+}, one phen, one $BTATz^{2-}$, one lattice water, and four coordinated water; the chemical formula can be described as Sr(BTATz)(phen)$(H_2O)_4 \cdot H_2O$. Strontium coordinates with two nitrogens (N1, N2) from phen, two nitrogens (N6 and N8) from $BTATz^{2-}$, and four oxygens (O1, O4, O5, and O8) from coordinated waters to form an eight-coordinate geometry (figure 3), as for **1**. The bond lengths between Sr and O (O1, $O4^{\#1}$, O5, and O8) are 2.536(6), 2.585(5), 2.610(4), and 2.622(4) Å, respectively. Distances between the strontium and nitrogens are not the same, 2.672 for Sr–N(6)#2, 2.735 for Sr–N(2)#1, 2.756 for Sr–N(1)#1, and 2.818 for Sr–N(8)#2, longer than the Sr–O bonds. Bond length of Sr–N(8)#2 is longer, showing that strontium is weakly coordinated with N(8)#2.

From the packing plot of Sr(BTATz)(phen)$(H_2O)_4 \cdot H_2O$ (figure 4), there are many hydrogen bonds because of the existence of N–H and O–H (table 2). The coordination bonds and the hydrogen bonds make the complex a polymer.

3.2. *Thermal decompositions*

To assess the thermal behaviors of **1** and **2**, thermal decomposition processes were investigated by DSC and TGA measurements.

The DSC and TG-DTG curves under linear heating rate of 10 K min^{-1} for **1** are shown in figures 5 and 6, respectively. In the DSC curve, there are two endothermic and one exothermic process from 300 to 820 K occurs. The first process occurs at 346–398 K, corresponding to the mass loss of 12.67% in the TG curve. Three lattice waters and three coordinated waters are lost from $Sr_2(BTATz)_2(H_2O)_8 \cdot 3H_2O$ on heating, consistent to theoretical calculation (12.59%). Different bond lengths of Sr–O (table 2) are not broken at the same time when the complex is heated.

The second endothermic process occurs from 409 to 472 K with the peak maximum temperature (T_p) of 436 K. In TG-DTG curves, another mass loss of 6.23% is observed, which is close to the calculated value of 6.29% for loss of the other three coordinated waters.

Downloaded by [Renmin University of China] at 10:48 13 October 2013

Downloaded by [Renmin University of China] at 10:48 13 October 2013

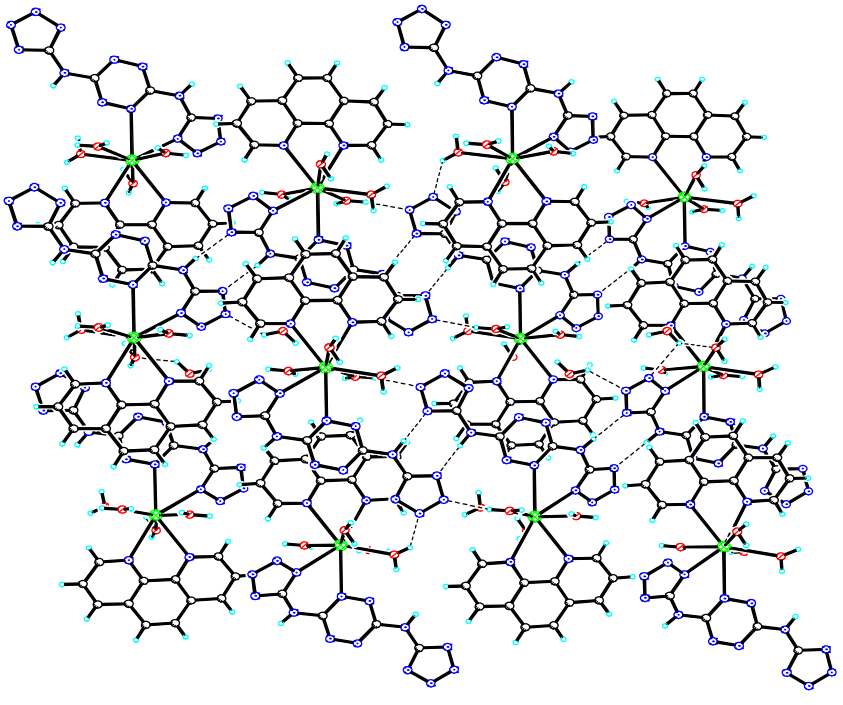

Figure 4. Packing diagram of **2** viewed along the *a*-axis.

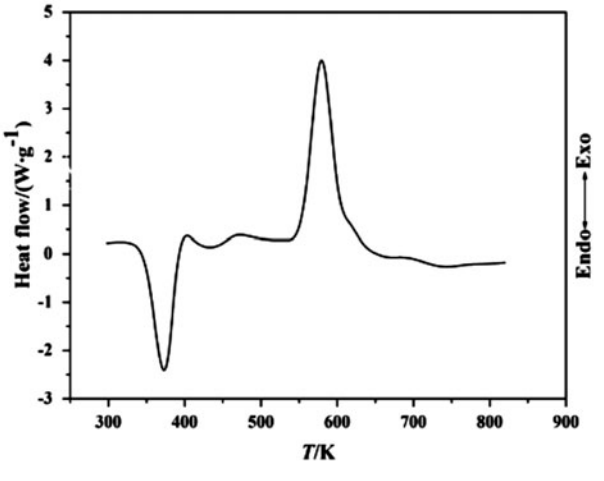

Figure 5. DSC curve of **1** at a heating rate of 10 K min^{-1}.

With the temperature increasing, the exothermic decomposition process begins at 556–658 K with the peak temperature 579.18 K; the exothermic enthalpy is 713 kJ mol^{-1}. Corresponding to this exothermic process, there is a main mass loss of 28.08% in the TG-DTG curves caused by the violent decomposition of $BTATz^{2-}$.

DSC and TG-DTG curves of **2** are shown in figures 7 and 8, respectively. There are also two endothermic and one exothermic process in the DSC curve between 300 and

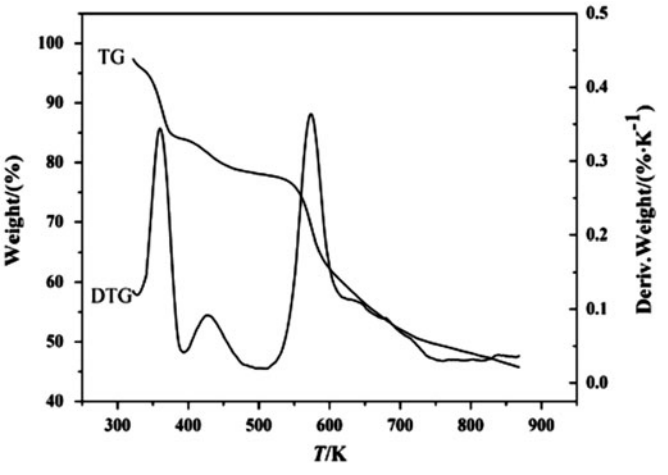

Figure 6. TG-DTG curves of **1** at a heating rate of 10 K min^{-1}.

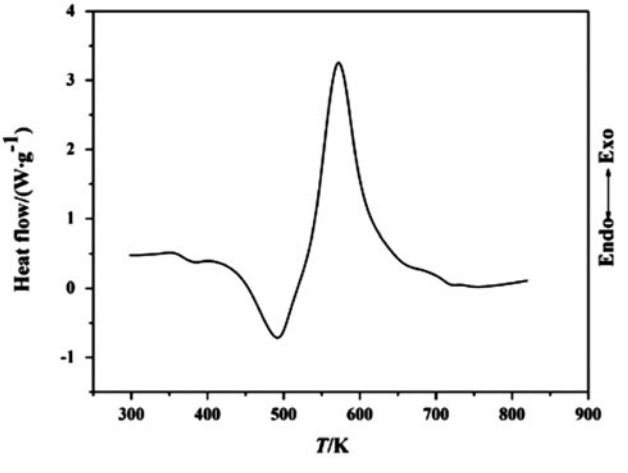

Figure 7. DSC curve of **2** at a heating rate of 10 K min^{-1}.

820 K with the second endothermic process stronger than the first one. The first exothermal process is at 363–403 K, with mass loss of 4.99% in TG-DTG curves, caused by the loss of one lattice water and one coordinated water (Calcd 5.29%).

The two successive endothermic processes occur between 380 and 490 K in the DSC curve (figure 7), corresponding to two mass loss processes in the TG-DTG curves. The second mass loss of 8.67% at 430–490 K is from losing the other four coordinated waters (calculated 8.94%).

Decomposition of 1,10-phen is higher than that of the BTATz [9,21], so the last mass loss of 29.36% at 520–730 K could be assigned to decomposition of $BTATz^{2-}$ (calculated 29.83%). The exothermic decomposition enthalpy of this process is 560 kJ mol^{-1}, lower than that of **1**.

Downloaded by [Renmin University of China] at 10:48 13 October 2013

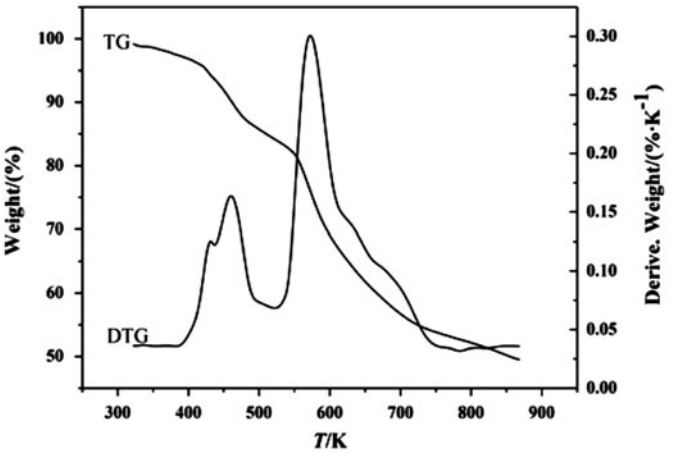

Figure 8. TG-DTG curves of **2** at a heating rate of 10 K min^{-1}.

3.3. *Non-isothermal kinetic analysis*

To explore the decomposition mechanisms of **1** and **2** and obtain the corresponding kinetic parameters [apparent activation energy (E_a/kJmol^{-1}), pre-exponential constant (A/s^{-1})], a multiple heating method (Kissinger method [22] and Ozawa method [23]) was employed. The Kissinger and Ozawa equations [equations (1) and (2)] are as follows:

$$\frac{d\ln(\beta/T_p^2)}{d(1/T_p)} = -\frac{E_a}{R} \tag{1}$$

$$\log\beta + \frac{0.4567E_a}{RT_p} = C \tag{2}$$

where β is the linear heating rate, T_P is the peak temperature, A is the pre-exponential constant, R is the gas constant, E is the apparent activation energy, and C is a constant.

The main exothermic process makes a dominant effect on the decomposition of energetic materials. Based on the DSC curves obtained under the conditions of static air at four different heating rates of 5, 10, 15, and 20 K min^{-1}, the values of the peak temperature T_p (K); the apparent activation energies E_k and E_o (kJ mol^{-1}), where subscript k and o are the methods of Kissinger and Ozawa, respectively; the pre-exponential constant (A/s^{-1}) and linear coefficients (r_k and r_o) were also determined by the two methods. Values of T_{e0} and T_{p0} corresponding to $\beta \to 0$ are obtained by equation (3). The detailed data and calculated kinetic parameters are listed in table 4.

$$T_{(0,\mathrm{eorp})i} = T_{(00,\mathrm{e0orp0})} + n\beta_i + m\beta_i^2 i = 1\text{–}4 \tag{3}$$

where n and m are coefficients.

Downloaded by [Renmin University of China] at 10:48 13 October 2013

Table 4. Basic data for the main exothermic decomposition processes of **1**, **2** and BTATz.

	β/(K min^{-1})	T_e/K	T_p/K	E_{pk} (kJ mol^{-1})	lnA_k [A/(s^{-1})]	r_k	E_O/(kJ mol^{-1})		r_o	T_{e0}/K	T_{p0}/K
							E_{eo}	E_{po}			
1	5	552.11	570.81	199.07	16.03	0.9843	193.67	198.48	0.9857	542.33	564.02
	10	559.74	578.94								
	15	565.92	582.80								
	20	569.72	589.87								
2	5	531.41	564.55	203.92	16.68	0.9985	201.79	202.97	0.9986	523.96	554.46
	10	537.39	572.41								
	15	543.12	578.45								
	20	546.97	582.12								
BTATz	5	578.29	588.90	249.08	19.97	0.9942	247.34	246.30	0.9946	567.75	581.61
	10	585.41	595.34								
	15	591.14	600.40								
	20	592.77	604.79								

From table 4, the calculated results using both the methods correspond with each other and are in the normal range of solid materials [24]. The apparent activation energy of the two complexes is close, which corresponds to the onset temperature (T_e) of the DSC curve.

In order to further estimate the rate constant of the initial decomposition process of the two complexes and also determine their thermal decomposition mechanism, the Arrhenius equation can be used, expressed by using the calculated E_a (the average of E_{pk} and E_{po}) and ln A_k as follows: ln $k = 16.03 – 198.78 \times 10^3/RT$, ln $k = 16.68 – 203.45 \times 10^3/RT$.

3.4. *Thermal safety*

Research focuses on energetic materials is not only for seeking high energy but also considering thermal safety. Values of self-accelerating decomposition temperature (T_{SADT}), the thermal ignition temperature (T_{be0} or T_{TIT}), the critical temperature of thermal explosion (T_b), and the adiabatic time-to-explosion (t_{TIad}) could be used to estimate thermal safety.

According to the data of table 4, these parameters can be obtained by equations (4) and (5) [24–26], where E_O is the apparent activation energy obtained by Ozawa's method. The T_{be0} or T_{TIT} is obtained by substituting E_{eO} and T_{e0} into Zhang–Hu–Xie–Li equation (5) [27]. The critical temperatures of thermal explosion (T_{bp0} or T_b) is obtained by substituting E_{pO} and T_{p0} into the equation

$$T_{SADT} = T_{e0} \tag{4}$$

$$T_{be0(orbp0)} = \frac{E_O - \sqrt{E_O^2 - 4E_O R T_{e0(orp0)}}}{2R} \tag{5}$$

The adiabatic time-to-explosion (t_{TIad}) of energetic materials is the time of decomposition to explosion under adiabatic conditions; it is another important parameter for assessing thermal stability and safety. Substituting the following basic data into the Smith equation [equations (6)–(8)] [28, 29], the value of t_{TIad} could be obtained.

Downloaded by [Renmin University of China] at 10:48 13 October 2013

$$C_p \frac{dT}{dt} QA \exp(-E/RT) f(\alpha) \tag{6}$$

$$t_{TIad} = \int_0^t dt = \frac{1}{Q_d A} \int_{T_{e0}}^{T_b} \frac{C_p \exp(E/RT)}{f(\alpha)} dT \tag{7}$$

$$\alpha = \int_{T_{e0}}^{T_b} \frac{C_p}{Q_d} dT \tag{8}$$

For **1**: $C_p(Jg^{-1}K^{-1}) = 4.1528 \times 10^{-3} + 4.0523 \times 10^{-3} T$, $Q_d = 675.67\,J\,g^{-1}$, $E = E_K = 199{,}070\,JM^{-1}$, $A = A_K = 10^{16.03}$, $R = 8.314\,JM^{-1}K^{-1}$, mechanism function $f(\alpha) = (1-\alpha)^2$, the integral lower limit $T_{eo} = 542.33\,K$, the upper limit $T_b = 578.02\,K$.

For **2**: $C_p(Jg^{-1}K^{-1}) = 0.48186 + 4.3594 \times 10^{-3} T$, $Q_d = 958.18\,Jg^{-1}$, $E = E_K = 203{,}920\,JM^{-1}$, $A = A_K = 10^{16.68}$, $R = 8.314\,Jmol^{-1}K^{-1}$, mechanism function $f(\alpha) = (1-\alpha)^2$, the integral lower limit $T_{eo} = 523.96\,K$, the upper limit $T_b = 567.66\,K$.

The entropy of activation ($\Delta S^{\neq}$), enthalpy of activation ($\Delta H^{\neq}$), and free energy of activation ($\Delta G^{\neq}$) of the main exothermic decomposition reaction of the propellant, corresponding to $T = T_{p0}$, $E_a = E_{pk}$, and $A = A_k$, are obtained by equations (9)–(11) [23–25]

$$A = (k_B T/h)\, e^{\Delta S^{\neq}/R} \tag{9}$$

$$\Delta H^{\neq} = E - RT \tag{10}$$

$$\Delta G^{\neq} = \Delta H^{\neq} - T\Delta S^{\neq} \tag{11}$$

where k_B is the Boltzmann constant ($1.3807 \times 10^{-23}\,JK^{-1}$) and h is the Planck constant ($6.625 \times 10^{-34}\,Js^{-1}$).

The values of T_{SADT}, T_{TIT}, T_b, t_{TIad}, $\Delta S^{\neq}$, $\Delta H^{\neq}$, and $\Delta G^{\neq}$ for **1** and **2** are summarized in table 5. From the results (table 5), values of the temperature for **1** are higher than that of **2**. However, the theoretical value (t_{TIad}) of **1** is lower than **2**, which can be explained by C_p. C_p of 1 is obviously lower than **2** at the same temperature, but the E_{pk} of the two complexes is similar. Because the bond lengths of Sr–O and Sr–N are longer than N–N, C–N, and N=N, BTATz is little more stable than **1** and **2**, and much more stable than RDX [30, 31]. Comparing the data listed in table 5, it can be deduced that the order of thermal stability is BTATz > 1 > 2 > RDX.

Table 5. The derivative parameters for **1**, **2**, BTATz and RDX.

	1	**2**	BTATz	RDX
T_{SADT}/K	542.23	523.96	567.75	477.15
T_{TIT}/K	555.58	535.79	579.02	482.13
T_b/K	578.02	567.66	593.50	490.55
t_{TIad}/s	71.93	196.47	27.13	3.19
$\Delta S^{\neq}$/(J mol^{-1} K^{-1})	56.66	69.25	131.83	177.39
$\Delta H^{\neq}$/(kJ mol^{-1})	194.38	199.31	244.24	48.96
$\Delta G^{\neq}$/(kJ mol^{-1})	162.42	160.91	167.57	−36.54

Downloaded by [Renmin University of China] at 10:48 13 October 2013

4. Conclusions

Two new high-energy metal complexes, $Sr_2(BTATz)_2(H_2O)_8 \cdot 3H_2O$ and Sr(BTATz)(phen)$(H_2O)_4 \cdot H_2O$, were synthesized and characterized by IR, elemental analysis and single crystal X-ray diffraction. Strontium is eight-coordinate for both the complexes. There are two endothermic processes and an intensely exothermic process for both of them in DSC and TG-DTG curves. The decomposition temperature of **1** (549 K) and **2** (532 K) are little higher than that of $[Mg(CHZ)_3](ClO_4)_2$ (530 K) [32] and $[Bi(tza)_3]_n$ (517 K) [33]. That is, the former two complexes are more stable than the latter. The exothermic enthalpy of **1** is 713 kJ mol^{-1}, which is close to that of the complex of $[Bi(tza)_3]_n$ (714 kJ mol^{-1}) [33]. So, the title two complexes have enormous potential as energetic materials. The Arrhenius equation for **1** and **2** can be expressed as: $\ln k = 16.03–198.78 \times 10^3/RT$ and $\ln k = 16.68–203.45 \times 10^3/RT$, respectively. The T_{SADT}, T_{TIT}, T_b, and t_{TIad} for the two complexes are calculated as 542, 556, and 578 K, 71.93 s; 524, 536, and 568 K, 196 s, respectively. The above mentioned data show that thermal safety of 1 has some advantage over **2**.

Downloaded by [Renmin University of China] at 10:48 13 October 2013

Supplementary material

CCDC-887783 (**1**) and CCDC-887784 (**2**) contain the supplementary crystallographic data for this article. These data can be obtained free of charge at www.ccdc.cam.ac.uk/conts/retrieving.htmL or from the Cambridge Crystallographic Data Center (CCDC), 12 Union Road, Cambridge, CB2, 1EZ, UK; Fax: +44 1223 336033; E-mail: deposit@ccdc.cam.ac.uk.

Acknowledgments

We thank the National Natural Science Foundation of China (21101127), the Natural Science Basic Research Plan in Shaanxi Province of China (2011JQ2002), China Postdoctoral Science Foundation funded project (20110491676), the National Defense Pre-Research Foundation of China (9140A28020111BQ3401) and the National Natural Science Foundation of China (21073141).

References

[1] M.A. Hiskey, D.E. Chavez, D. Naud. *US Patent* 6342589 (2002).
[2] M.A. Hickey, D.E. Chavez, D. Naud. *US Patent* 6657059 (2003).
[3] A. Saikia, R. Sivabalan, B.G. Polke, G.M. Gore, A. Singh, A.S. Rao, A.K. Sikder. *J. Hazard. Mater.*, **170**, 306 (2009).
[4] X.G. Zhang, H. Zhu, S.Q. Yang, W. Zhang, F.Q. Zhao, Z.R. Liu, Q. Pan. *Chin. J. Propul. Technol.*, **28**, 322 (2007).
[5] M.A. Hiskey, A. Michael, D.E. Chavez. *US Patent* 6458227 (2002).
[6] S.F. Son, H.L. Berghout, C.A. Bolme, D.E. Chavez, D. Naud, M.A. Hiskey. *Proc. Combust. Inst.*, **28**, 919 (2000).
[7] S.T. Yue, S.Q. Yang. *Chin. J. Energ. Mater.*, **12**, 155 (2004).
[8] B.Z. Wang, W.P. Lai, Q. Li, P. Lian, Y.Q. Xue. *Chin. J. Org. Chem.*, **28**, 422 (2008).
[9] J.H. Yi, F.Q. Zhao, W.L. Hong, S.Y. Xu, R.Z. Hu, Z.Q. Chen, L.Y. Zhang. *J. Hazard. Mater.*, **176**, 257 (2010).
[10] F.Q. Zhao, P. Chen, S.W. Li, B.C. Wang, H. Du, M.Z. Deng. *Acta Armamentaria*, **25**, 30 (2004).

[11] J.C. Song, T.L. Zhang, J.G. Zhang, Y.F. Li, G.X. Ma, K. Chin. *J. Struct. Chem.*, **23**, 347 (2004).
[12] X.Z. Fan, J.Z. Li, L.Y. Zhang, B.Z. Wang, X.G. Liu. *Chin. J. Energ. Mater.*, **15**, 316 (2007).
[13] Y.H. Ren, J.H. Yi, F.Q. Zhao, Z.Q. Chen, R.Z. Hu, J.R. Song. *Chin. J. Explos. Propel.*, **33**, 19 (2010).
[14] H.X. Gao, J.M. Shreeve. *Chem. Rev.*, **111**, 7377 (2011).
[15] H.Y. Chen, T.L. Zhang, J.G. Zhang, L. Yang. *Chin. J. Energ. Mater.*, **14**, 21 (2006).
[16] H. Wang, F.Q. Zhao, S.W. Li, H.X. Gao. *Chin. J. Explos. Propel.*, **29**, 32 (2006).
[17] G.M. Sheldrick. *SHELXL-97, Program for the Refining of Crystal Structure*, University of Gottingen, Germany (1997).
[18] Y.M. Yang, T.L. Zhang, J.G. Zhang. *Chin. J. Struct. Chem.*, **21**, 321 (2002).
[19] H. Zhang, T.L. Zhang, J.G. Zhang, X.J. Qiao, L. Yang, Y.H. Sun. *Chin. J. Inorg. Chem.*, **22**, 346 (2006).
[20] Y. Hu, Y.H. Shao, R.Z. Hu, J.R. Song, H.X. Ma. *Chin. J. Energ. Mater.*, **20**, 273 (2012).
[21] E.L. Yang, N. Zhang, Z.M. Shan, Y.L. Wang, H.C. Hu, Q.Y. Liu. *Chin. J. Struct. Chem.*, **30**, 196 (2011).
[22] H.E. Kissinger. *Anal. Chem.*, **19**, 1702 (1957).
[23] T. Ozawa. *Bull. Chem. Soc. Jpn.*, **38**, 1881 (1965).
[24] R.Z. Hu, S.L. Gao, F.Q. Zhao, Q.Z. Shi, T.L. Zhang, J.J. Zhang. *Therm. Anal. Kinet*. (in Chinese), 2nd Edn Edn, Science Press, Beijing (2008).
[25] J.H. Yi, F.Q. Zhao, H.X. Gao, S.Y. Xu, M.C. Wang, R.Z. Hu. *J. Hazard. Mater.*, **153**, 261 (2008).
[26] F.Q. Zhao, R.Z. Hu, H.X. Gao, H.X. Ma. In *New Developments in Hazardous Materials Research*, O.E. Bronna (Ed.), Chap. 4, pp. 161–167, Nova Science Publishers Inc., New York (2006).
[27] T.L. Zhang, R.Z. Hu, Y. Xie, F.P. Li. *Thermochim. Acta*, **244**, 171 (1994).
[28] L.C. Smith. *Thermochim. Acta*, **13**, 1 (1975).
[29] R.Z. Hu, H. Zhang, Z.M. Xia, P.J. Guo, S.L. Gao, Q.Z. Shi, G.E. Lu, J.Y. Jiang. *Chin. J. Energ. Mater.*, **11**, 130 (2003).
[30] Z. Tang, Y. Ren, L. Yang, T.L. Zhang, X.J. Qiao, J.G. Zhang, Z.N. Zhou. *Chin. J. Explos. Propel.*, **34**, 19 (2011).
[31] K.Z. Xu, C.R. Cahng, J.R. Song, H.X. Gao, M. Li. *Chin. J. Explos. Propel.*, **31**, 35 (2008).
[32] Z.M. Li, T.L. Zhang, L. Yang, Z.N. Zhou, J.G. Zhang. *J. Coord. Chem.*, **65**, 143 (2011).
[33] S.W. Wang, L. Yang, T.L. Zhang, G.T. Zhang, J.G. Zhang, Z.N. Zhou. *J. Coord. Chem.*, **64**, 2583 (2011).

Downloaded by [Renmin University of China] at 10:48 13 October 2013